

Igneous Diversity of the Early Martian Crust

Valerie Payré ^{1,*} , Arya Udry ² and Abigail A. Fraeman ³

¹ Department of Earth and Environmental Sciences, University of Iowa, Iowa City, IA 52242, USA

² Department of Geoscience, University of Nevada Las Vegas, Las Vegas, NV 89154, USA; arya.udry@unlv.edu

³ Jet Propulsion Laboratory, California Institute of Technology, Pasadena, CA 91109, USA; abigail.a.fraeman@jpl.nasa.gov

* Correspondence: valerie-payre@uiowa.edu; Tel.: +1-319-467-1546

Abstract: Mars missions and Martian meteorites revealed how complex the Martian crust is. The occurrence of both alkaline and sub-alkaline igneous rocks of Noachian age (>3.7 Ga) in Gale crater indicates diverse magmatic processes, with sub-alkaline rocks likely formed through the partial melting of hydrous mafic rocks, as commonly observed on Earth. The orbital discovery of excavated evolved igneous rocks scattered in Noachian terrains raise questions about the petrology of the ancient Martian crust, long thought to be basaltic. A possibly evolved crust beneath a mafic cover is supported by geophysical and seismic measurements from the *Insight* lander that indicate the bulk crust has a lower density than expected if it were homogeneously basaltic. If localized magmatic processes could form evolved terrains, the detection of abundant intermediate to felsic Noachian crustal exposures through remote sensing suggest regional- to global-scale processes that produced evolved crustal component(s) that are now buried below mafic materials. Due to the lack of centimetric to millimetric textural imaging and compositional measurements, the petrology of such crust is ambiguous. Future orbiter, rover, and aerial missions should focus on Noachian exposed regions exhibiting evolved crustal characteristics to unfold the petrology of the Martian crust and its formation.

Keywords: Mars; crust; petrology; missions; helicopter; sub-alkaline; alkaline; evolved; feldspar; pyroxene



Citation: Payré, V.; Udry, A.; Fraeman, A.A. Igneous Diversity of the Early Martian Crust. *Minerals* **2024**, *14*, 452. <https://doi.org/10.3390/min14050452>

Academic Editor: Kattathu Mathew

Received: 7 January 2024

Revised: 19 April 2024

Accepted: 23 April 2024

Published: 25 April 2024



Copyright: © 2024 by the authors. Licensee MDPI, Basel, Switzerland. This article is an open access article distributed under the terms and conditions of the Creative Commons Attribution (CC BY) license (<https://creativecommons.org/licenses/by/4.0/>).

1. Introduction

Mars' crust was long thought to be homogeneously basaltic, but data acquired by Martian meteorites, rovers, and orbiters this last decade questioned this assumption by revealing an unexpected diversity of igneous rocks [1,2]. Most Martian meteorites are young (<2.4 Ga) and belong to the shergottite–nakhlite–chassignite (SNC) group. SNCs have mafic compositions ($\text{SiO}_2 < 52$ wt.%), with basaltic and gabbroic sub-groups, as well as olivine and pyroxene cumulates, respectively (e.g., [3–7] and references therein). Yet, the most ancient igneous clasts, discovered in a Martian meteorite called Northwest Africa (NWA) 7034 and its paired rocks dated at 4.41 Ga [8], have basaltic to trachytic and monzonitic compositions [9–12]. Igneous rocks analyzed by the Mars Exploration Rover (MER) *Spirit* evidenced Hesperian (3.0–3.7 Ga) olivine-rich basalts and alkaline basalts, while the *Curiosity* rover analyzed Noachian (>3.7 Ga) igneous rocks of diverse textures and compositions, from mafic ($\text{SiO}_2 < 52$ wt.%) to alkaline and sub-alkaline intermediate ($\text{SiO}_2 = 52\text{--}62$ wt.%) and felsic ($\text{SiO}_2 > 62$ wt.%) rocks (Figure 1; [13,14]). Similarly to [1,13–15], igneous rocks are qualified as alkaline and sub-alkaline, when their composition in the TAS diagram is plotting above and below the Irvine–Baragar line (red line in Figure 1). The detection of an alkaline and sub-alkaline suite (Figure 1) on Mars is of importance because it highlights different magmatic processes occurring in the vicinity of Gale crater as emphasized in [1]. Global-scale remote sensing observations show a surface covered by mafic igneous minerals including olivine, pyroxene, and plagioclase (e.g., [16,17]), but several terrains exposed at the surface by impacts, tectonics, or erosional

processes present feldspar-rich (>60 vol.%) signatures of evolved compositions (defined here as intermediate and felsic; [18–20]).

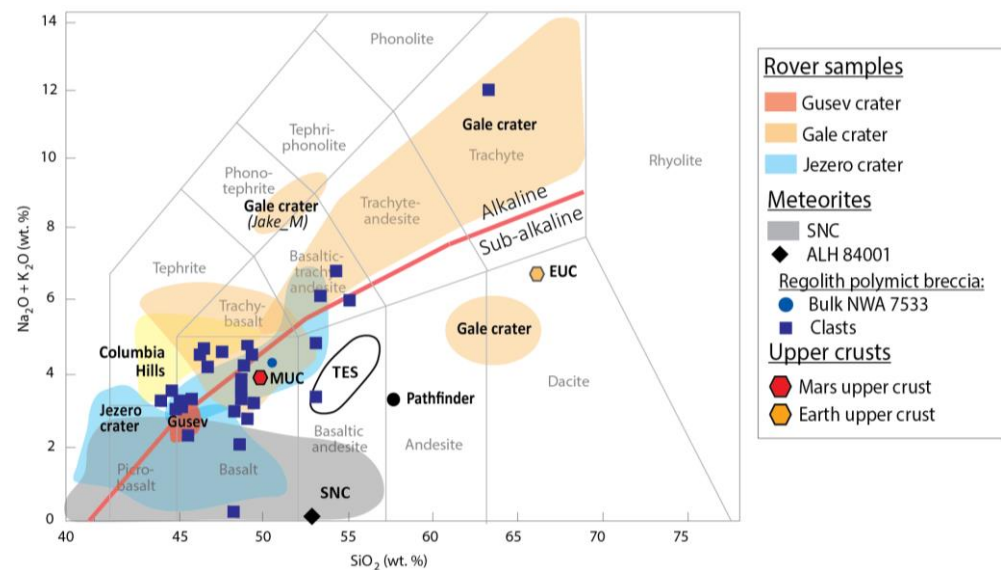


Figure 1. Total alkali silica (TAS) diagram showing the composition of igneous rocks analyzed by Mars rovers and within Martian meteorites [3,9–14,21–24]. Compositions deduced from the global mineralogy measured by the Thermal Emission Spectrometer (TES) onboard the Mars Global Surveyor spacecraft are circled in black (from [25]). The mineralogy estimated with TES is based on non-partial least squares deconvolution models using an end-member library [26]. Using the composition of the minerals in the library, the composition of the Martian surface was deduced (details in [25]). The composition of the upper crust from Earth (orange polygon) and Mars (red polygon) are added for reference [25,27]. The red line corresponds to the limit between alkaline and sub-alkaline igneous rocks [28].

All the datasets we currently have from Mars emphasize the presence of diverse igneous rocks and terrains of Noachian age, raising questions about the composition and formation of the early Martian crust. While pockets of evolved terrains might have formed following magmatic processes such as the fractional crystallization of basaltic melts at localized regions [29,30], the fact that they are found in exposed surface could suggest a buried evolved crust covered by subsequent younger basaltic materials [1,15,20,31]. This latter hypothesis is supported by crustal density estimates derived from geoid-to-topography ratios and seismic data that are too low to represent an entirely basaltic crust [32,33], and seismic data suggesting andesitic crustal compositions [34]. If the early Martian crust was composed of evolved crustal components as suggested occurring at Terra Cimmeria and Sirenum [20,35,36], its formation mechanism still needs to be constrained. This article reviews the most up-to-date detections of Noachian igneous materials at the surface of Mars, and describes the formation processes of alkaline and sub-alkaline evolved igneous rocks presented in the literature, as well as the composition and potential formation mechanisms of the early Martian crust. Key observations and guidance for current and future missions to Mars are provided to enlighten us on the composition of the early Martian crust.

2. Igneous Diversity in Martian Datasets

Martian meteorites, and igneous clasts and rocks analyzed by rovers and orbiters suggest diverse compositions of Noachian magmas. This section reviews such igneous materials dated from Noachian time (>3.7 Ga).

2.1. Martian Meteorites

Currently, 374 individual Martian meteorites—corresponding to 246 paired groups—have been classified. All but two of these specimens are younger than 2.4 Ga and are known as the shergottite–nakhlite–chassignite (SNC) group (Meteoritical Bulletin; see [3] for a review on Martian meteorites). The first recovered Noachian Martian rock (in 1984) is Allan Hills (ALH) 84001, which shows a Lu–Hf crystallization age of ~4.1 Ga [37]. This meteorite is an orthopyroxenite and consists of large 4–5 mm anhedral orthopyroxenes with triple-junction grain boundaries, euhedral to subhedral chromite, maskelynite, and minor augite, apatite, pyrite, carbonates, and olivine [38,39]. The orthopyroxene compositions are homogeneous throughout the sample, with an average composition of $Wo_3En_{70}Fs_{27}$ [38]. Minor silica, sometimes seen as quartz and tridymite grains, were also observed [40]. Differing from most Martian meteorites, it has undergone different shock events [33]. This meteorite also contains secondary Fe–Mg–Mn–carbonates and magnetite [41,42]. ALH 84001's texture and mineralogy indicate that it underwent slow cooling and is likely a cumulate that originated from a basaltic parental magma [38,39]. ALH 84001 resembles the enriched shergottite isotopic mantle reservoir, shergottites being the most common type of Martian meteorites [3]. A source age of ~20 Ma after calcium aluminum inclusion (CAI) condensation was found by [43].

Northwest Africa (NWA) 7034 and its 17 paired meteorites (including NWA 7533), also commonly called Black Beauty, is the only breccia in the Martian meteorite collection and represents Noachian processes. The visible/near-infrared (VNIR) spectral properties of this meteorite resemble those of the average Noachian crust [44]. It consists of different types of clasts from igneous, sedimentary, and impact origins set in a microcrystalline (~1 μ m) matrix containing single mineral fragments, mostly plagioclase and pyroxene [9–12,45–47]. The different clasts have been classified by texture and mineralogy (see [9,10,12,47,48]), as well as compositions [11,45]. Compositions such as basaltic, basalt–andesitic, trachyandesitic, and Fe–Ti–P-rich clasts, with varying textures from fine-grained (microbasalts, and sedimentary clasts) and medium-grained (noritic and monzonitic clasts) were analyzed (e.g., [9]; Figure 1). Some of the melt clasts are classified as clast-laden impact melt rock (CLIMR), consisting of fine lithic and crystal fragments [9,10]. In terms of mineralogy, this breccia includes pyroxene, plagioclase, K-feldspar, phosphates, ilmenite, zircons, and baddeleyite. Orthopyroxenes are present in all clasts ($Wo_{2-3}En_{74-44}Fs_{24-54}$ in mafic clasts and $Wo_{0-4}En_{47-77}Fs_{22-50}$ in evolved clasts); augite ($Wo_{41-48}En_{33-45}Fs_{20-50}$) and pigeonite ($Wo_{6-10}En_{28-57}Fs_{35-64}$) are also present in basaltic and trachyandesitic clasts with Mg number (Mg#), or molar $100 \times Mg/(Fe+Mg)$, varying from ~49 to 62 and ~33 to 57, respectively [10,11]. Plagioclase is found in all clasts (An_{30-50} and An_{10-30} in mafic and felsic clasts, respectively), and alkali feldspar (Or_{70-90}) is mostly observed in felsic clasts. Surprisingly, olivine, which is present in most Martian meteorites, is largely absent from this rock and only present in some impact melt clasts [49]. The dearth of olivine might be due various reasons including high oxygen fugacity fO_2 in the parental magmas shifting the olivine–orthopyroxene peritectic to a lower SiO_2 as suggested by a fO_2 between the fayalite–magnetite–quartz (FMQ) buffer –1 and FMQ +4 [11], or high degrees of partial melting in early Mars compared to later Mars, which would inhibit the crystallization of olivine [50]. The breccia is the only Martian meteorite showing evolved bulk compositions with both high alkalis and SiO_2 compositions, although evolved pockets representing extensive fractional crystallization are present in the 174 Ma gabbroic shergottite NWA 6963 [51,52].

The different clasts have variable mineralogies and compositions, showing that they do not originate from the same parental magmas and have undergone different degrees of fractionation [4,5]. Their different texture and mineralogy (aphanitic versus phaneritic texture, as well as the occurrence of pyroxene exsolutions) show that these clasts represent intrusive and extrusive processes, both magmatic- and impact-related. It is possible that all the clasts in NWA 7034, even those emplaced at depth, have undergone impact processes

based on the high concentration of platinum group elements and siderophile elements, potentially indicating ~5% of the additional asteroidal component in this rock [10,12,53].

The NWA 7034 clasts are the oldest Martian material ever dated. Zircons with U-Pb and Pb-Pb crystallization ages > 4.3 Ga were analyzed with ages of up to 4485.5 ± 2.2 down to 4300 ± 0.08 Ma [8,46,54–56]. Ref. [54] analyzed >50 grains and observed a bimodal distribution of old ages for zircons of around 4474 ± 10 Ma and 4442 ± 17 Ma. Most of the measured grains were out of a geologic context, except for one zircon in an alkaline clast dated at 4.72 ± 0.23 Ga [46], and a zircon from a basalt clast dated at 4.442 ± 0.17 Ga. Although this age has a large error, it shows that evolved alkaline magmatism was already present on Mars very early during its history, within the first 200 Myr. The low $^{176}\text{Lu}/^{177}\text{Hf}$ and Sm/Nd isotopic compositions and rare earth element (REE) composition of Zr-bearing minerals suggest an enriched and andesitic primary crust, which has been reworked through impacts, with a source different from the enriched shergottite source [9,43,46,53,54,56,57]. Based on the Hf composition, Ref. [8] determined a crustal source with a possible andesitic composition with a minimum source model age of 4.547 Ga, signifying that the magma ocean was likely completely crystallized and, possibly, the primary crust on Mars was already formed 20 Myr after the formation of the solar system (the first solid grain formed in the solar system at ~4.567 Ga; [58]). The bimodal distribution of ages suggested by [54] could represent primary crust melting caused by the impact during at least two impact episodes, around 4.474 and 4.442 Ga. After the formation of the igneous clasts, the meteorite underwent a complicated thermal and shock history [53] or lithification event ≤ 225 Ma [59], and was ejected between 2 and 12 Ma, possibly from the Karratha crater located in Terra Sirenum/Cimmeria (TSC) Province [36].

Compared to the other Martian meteorites, ALH 84001 and the NWA 7034 pairing groups are much older. These rocks are at least 1.7 Gyr older than the oldest shergottites (~2.4 Ga; [60]). Both of these meteorites likely originated from the southern highlands [36,39], whereas most of the Martian meteorites were likely ejected from the Tharsis province, a much younger terrain [61]. Both contain large amounts of orthopyroxene and the NWA 7034 group presents mafic and evolved clasts that contrast with the mineralogy and composition of younger meteorites presenting mafic compositions.

2.2. Rover Analyses

The *Spirit* MER mission that landed in Gusev crater in 2004 analyzed olivine–phyric basaltic lava flows in the Hesperian-aged Gusev crater floor, as well as alkaline basalts, trachybasalts, and tephrites at the Columbia Hills outcrop (Figure 1; [21,22]). The age of the latter alkaline rocks is still unclear, being formed either through a central uplift of the Noachian crater floor [62] or a more recent infilling, postdating the formation of the Hesperian olivine–phyric lava flows [63]. Both of these types of rocks are younger than Noachian, suggesting that several episodes of magmatic processes likely reworked the Noachian crust.

The *Curiosity* rover landed in Gale crater in 2012 at the dichotomy between the northern lowlands and southern highlands. It analyzed the first Noachian intermediate and felsic igneous rocks ever observed by a mission on the ground. The 155 km-diameter Gale crater was formed by an impact in the early Hesperian within a 4.21 Ga basement [64,65]. To date, ~59 igneous rocks have been analyzed, and all of them are either float rocks or lithic clasts in sedimentary conglomerates rather than igneous outcrops. They were transported from the northwestern watershed to the crater floor [14]. Twenty-eight of these rocks are intermediate and felsic without any olivine crystal [14], including one feldspar cumulate and several porphyritic rocks with euhedral feldspar phenocrysts [14,30,66]. No felsic outcrops have been spotted by remote sensing within the Gale crater watershed and walls where the igneous rocks might have originated from [67,68].

In Gale crater, two magmatic suites of five groups of igneous rocks were identified with an alkaline trend from basalts to trachytes, and a sub-alkaline trend from basalts to diorites (Figure 1; see more details of this topic in [13,14]). Basalts and basanites are dark with

aphanitic textures and sometimes conchoidal fractures (Figure 2a). Most display feldspar microliths surrounded by a dark groundmass composed of Mg-pigeonite, and olivine is lacking. These rocks are Fe-rich with a Mg# ranging from 0.25 to 0.65. Trachybasalts and trachyandesites are porphyritic rocks with 45%–80% of millimetric to centimetric euhedral feldspar within a dark fine-grained mesostasis of Fe-augite composition (Figure 2b). The large size of the feldspar crystals enabled chemical analyses with laser-induced breakdown spectroscopy (LIBS) within the ChemCam instrumental suite, revealing oligoclase to andesine compositions. Trachytes are leucocratic rocks with no visible crystals and sometimes presenting a vesiculated texture (Figure 2c). The groundmass is dominated by alkali-feldspar compositions, and the bulk compositions show low Mg# (0.30). Some alkaline rocks are silica-undersaturated with nepheline modeled by the CIPW normalization, while two trachytes are quartz-normative (Meetinghouse and Sledgers rocks, which are close to the sub-alkaline alkaline line in the TAS diagram) [14,29]. Sub-alkaline felsic rocks are quartz-normative, classified by [13] as quartz-diorites, quartz-monzonites, and granodiorites depending on their texture and mineralogy. They are coarse leucocratic plutonic rocks presenting with > 5 mm light-toned feldspar of mainly andesine compositions, and ~1 mm gray translucent crystals, potentially quartz intergrown with pink coarse alkali-feldspar, as well as secondary dark Fe-rich augite (Figure 2d). These sub-alkaline rocks contain a low alkali concentration of ~5 wt.% for elevated SiO₂ compositions ranging from 62 to 65 wt.%.

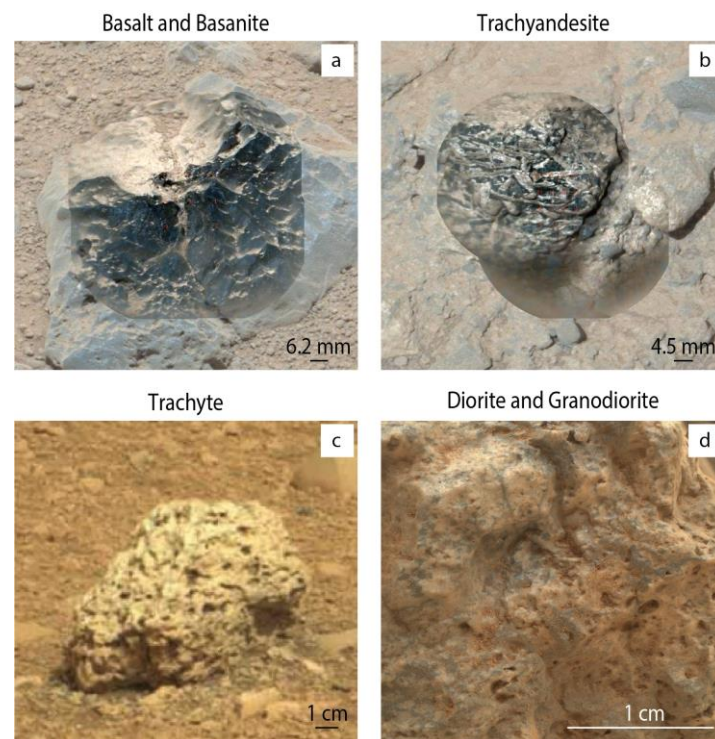


Figure 2. Images of Gale crater igneous rocks of the different categories discussed in the text. (a,b) Images of a basalt and trachyandesite, respectively, from the Remote Micro-Imager (RMI) part of the ChemCam suite onboard the *Curiosity* rover, superimposed on colored MastCam images. (c) MastCam image of a trachyte. (d) MAHLI image of a quartz-diorite.

Gale crater igneous rocks differ from igneous rocks analyzed by any other ground missions in that many of them are more evolved than mafic rocks and likely older. Both the *Spirit* and the *Perseverance* rovers that landed in Gusev and Jezero craters, respectively, identified basaltic to basalt–andesitic compositions of probably Hesperian age (Figure 1; [23,24]). The alkaline and sub-alkaline rocks in Gale crater are thought to be formed by different magmatic processes. Differentiation processes within a magma chamber, such as fractional crystallization of basaltic melts, crustal assimilation, and/or partial melting of a metasoma-

tized mantle, can explain the chemistry and mineralogy of alkaline evolved rocks [29–31,69]. Quartz-normative sub-alkaline evolved rocks might be formed similarly to those in most terrestrial settings, including partial melting of basalt and/or fractionation of basaltic melts with the presence of water [1,70]. Whether these igneous processes are local, regional, or global can be explored through remote sensing observation in Noachian terrains.

2.3. Remote Sensing Observations

Through VNIR spectroscopy analyzing the surface of Mars from orbit, the Noachian surface has been characterized by an elevated low-Ca pyroxene (LCP, orthopyroxene)/high-Ca pyroxene (HCP, pigeonite and augite) ratio, while LCP is nearly non-existent in Hesperian and Amazonian rocks [71,72]. Low-Ca pyroxene-rich massive outcrops were detected in excavated Noachian terrains, including the basement of Valles Marineris, as well as in various crater peaks in the southern highlands (Figure 3), suggesting the occurrence of LCP in the Noachian crust [73–75]. The transition from a higher to lower LCP/HCP ratio with time is also observed in Martian meteorites with the occurrence of orthopyroxene cumulates of Noachian ages in ALH 84001 and clasts in NWA 7034, compared to younger olivine- and/or augite-bearing Martian meteorites. An elevated degree of partial melting in early Mars due to a warm mantle has been suggested to produce LCP-rich igneous materials compared to mantle melting during the Hesperian and Amazonian age, when the partial melting of a cooler mantle resulted in the lack of LCP and an enhancement of olivine crystallizing [76].

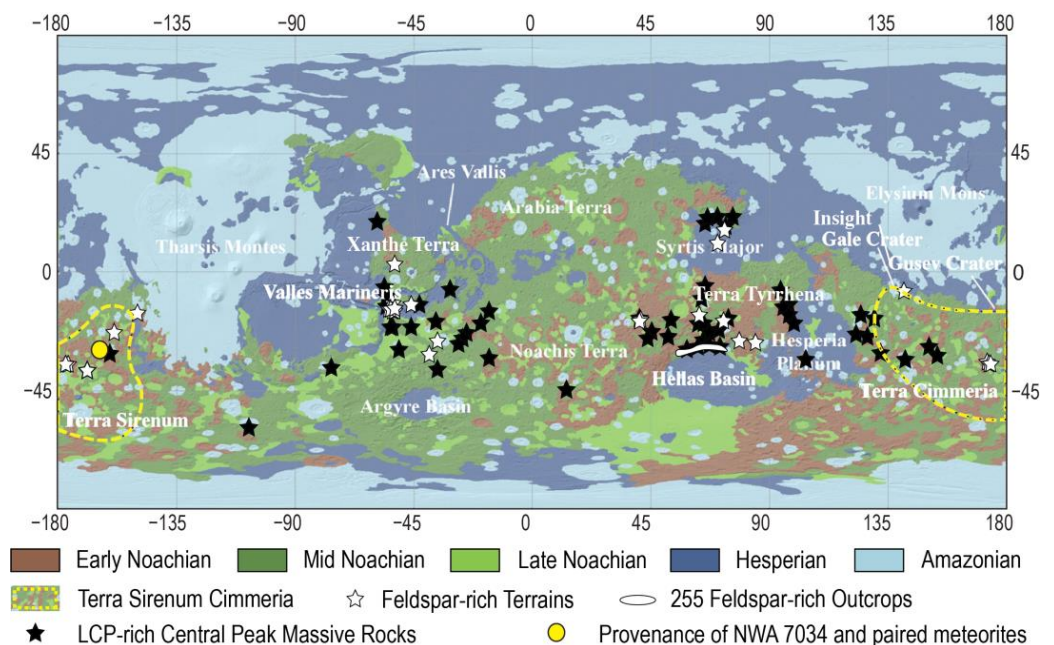


Figure 3. Geological map modified from [77] with the location of the feldspar-rich sites (white stars and regions; [18–20,78–80]), and LCP-rich central crater peak massive rocks (black stars; [75]). K-Th-rich terrain in the Terra Sirenum/Cimmeria region (yellow dashed line) is illustrated [35]. The ejection site of the Martian breccia NWA 7034 and its paired meteorites is indicated with a yellow circle [36].

In addition to an LCP-rich Noachian surface, several feldspar-rich terrains have been identified with VNIR spectroscopy using the Compact Reconnaissance Imaging Spectrometer of Mars (CRISM), onboard the Mars Reconnaissance Orbiter, especially in Noachian terrains (Figure 3; [18–20,78–80]). Reflectance VNIR spectroscopy is sensitive to absorptions caused by Fe-rich mafic minerals including olivine, orthopyroxene LCP, and clinopyroxene HCP, but phases expected in evolved rocks like quartz and Si-rich glass are spectrally neutral in that spectral range and difficult to identify. Plagioclase feldspar can be

detected, but only when Fe^{2+} is incorporated into the plagioclase lattice and the mineral is abundant compared to darker, spectrally dominant mafic phases (e.g., [81] and references therein). Considering the technique limitations, along with the lack of millimetric to centimetric images to characterize the texture, identifying the petrology of igneous terrains is challenging. Thermal emission spectroscopy with the Thermal Emission Imaging System (THEMIS) onboard the Mars Odyssey spacecraft is more sensitive to Si-rich phases, and data from this instrument can be used to estimate the silica concentration at the surface of Mars and provide indications of the mafic, intermediate, or felsic nature of the targeted non-altered igneous terrains. The wavelength of the weighed absorption center of the averaged THEMIS spectra over feldspar-rich terrains were calculated using the [82,83] approach as described in [20]. The THEMIS spatial resolution is 100 m/pixel, much coarser than CRISM's 18 m/pixel resolution and larger than the scale of many Martian outcrops. The silica concentration of feldspar terrains was thus estimated using THEMIS when the terrains were larger than the THEMIS spatial resolution.

Feldspar can be identified in the VNIR by a diagnostic absorption band at 1.25–1.30 μm characteristic of Fe^{2+} - Ca^{2+} substitutions in plagioclase feldspar. The ability to detect this absorption is also highly dependent on the texture, abundance, and setting of plagioclase feldspar [84]. Studies of powdered plagioclase feldspar mixed with basalt powder show the ~1.3 μm absorption is masked as plagioclase abundances < 90% [85], although feldspar can be detected in abundances as low as 30% when it is present as a phenocryst in igneous rocks [81]. Despite the challenging identification of feldspar, thorough analyses of excavated regions of Mars led to CRISM detections of absorptions attributed to feldspar in hundreds of locations within Noachian terrains, including nine at the Terra Sirenum/Cimmeria (TSC) region and hundreds in the northern walls of the Hellas basin (Figure 3). Most detections are located in regions exposed to the surface by impact, erosion, or fractures, including detections within crater rims, ejecta, fracture walls, or walls of eroded blocks, suggesting that feldspar-bearing terrains are older than the Noachian surface [20,78,79]. THEMIS analyses of these feldspar terrains suggest intermediate to felsic compositions (see details in [20]), supporting the occurrence of ancient evolved magmas early in Mars history. The petrology of these outcrops cannot be asserted due to the lack of close-up images and a complete mineralogy. They could either be bearing feldspar phenocrysts, similar to the porphyric trachyandesites and granodiorites found in Gale crater (Figure 2), or abundant microlitic feldspar volcanic materials. The evolved nature of the feldspar-bearing terrains recall intermediate and felsic rocks analyzed in Gale crater with feldspar abundances > 30% as phenocrysts in several rocks [14], and raise questions about whether these evolved outcrops are localized or occurring more globally in the Southern hemisphere below the surface. Without compositional analyses, these feldspar outcrops cannot be classified as alkaline or sub-alkaline.

Ref. [35] identified the TSC region as one of the most ancient regions of Mars (>4.2 Ga) with a relatively thick crust compared to other terrains at the surface of Mars (Figure 3). Magnetic anomalies are the most prominent in that region, and K and Th concentrations are more elevated than the surroundings, potentially suggesting more evolved terrains. The discovery of feldspar-rich terrains of intermediate compositions within cratered, eroded, and fractured terrains support the presence of an ancient evolved crustal component at TSC [20]. Moreover, Gale crater, where the most ancient evolved igneous rocks were found by a ground mission, is located on the northwestern boundary of TSC, and the crater which NWA 7034 and its paired meteorites were ejected from is hypothesized to be located within TSC (yellow circle in Figure 3; [36]). All this evidence from various datasets leans towards the occurrence of an evolved crust in the TSC region. The presence of additional feldspar-rich terrains of evolved composition elsewhere on Mars might be related to either a more global evolved crust, or other crustal/mantle processes that produced evolved magmatic pockets in some regions (e.g., potential impact-generated melts that crystallized feldspar-rich evolved rocks within the crater floor in Noachis Terra [19]).

The lack of high-resolution analyses and images of the evolved feldspar-rich and LCP-rich terrains prevent their petrological characterization. Future missions to Mars targeting these regions are of importance to inform the extent of the occurrence of alkaline and sub-alkaline igneous terrains, as well as their formation processes.

3. Discussion

3.1. Formation of Alkali and Sub-Alkali Evolved Rocks in Gale Crater

As discussed in detail in [1], alkaline and sub-alkaline rocks analyzed in Gale crater likely formed through different magmatic processes. To summarize, alkaline evolved rocks (trachyandesite, trachytes, and monzonites) cannot be formed directly by partial melting of a primitive mantle composition as illustrated by piston-cylinder experiments [86]. The mantle-derived melts would contain SiO₂ concentrations that are too low to match that of the trachyandesites and trachytes found in Gale. Partial melting of a K-metasomatized source [69,87] or fractional crystallization of a mantle-derived melt at low extents of melting (<14%; [13,29,30]) possibly associated with crustal assimilation [31] are processes that thermodynamical models and terrestrial analogs suggest could be possible. The differentiation of a magma or an impact melt sheet could also result in heavy minerals like LCP sinking in the bottom, leaving behind an alkaline-rich residual melt [15]. This could be consistent with the remote sensing observations of LCP- and feldspar-bearing terrains at the same location, although the geological contact is not always observed. All the options suggest an alkaline component at depth or within the crust, which can be achieved through a metasomatic mantle source or related to a Na- and K-rich primitive mantle compared to Earth's [15,88].

The presence of sub-alkaline evolved rocks indicate a hydrated mafic crust that was partially melted and/or subjected to the fractional crystallization of basaltic magmas in the presence of volatiles, as commonly observed in terrestrial settings [70]. On Earth, granodiorites similar to those observed in Gale crater are mainly found above subduction zones and volcanic arcs, and andesitic compositions can also occur in hot-spot rift settings like in Iceland (e.g., [89]). The assimilation of a hydrated basaltic crust during the fractional crystallization of magmas is a process that has been suggested to form terrestrial andesitic icelandites [89,90]. Hydrated sub-alkaline magmas are mainly related to the subduction of seawater stored within the crystal structure of altered rocks on the seafloor and the dehydration of the subducted slab, which leads to partial melting of the mantle wedge and/or of the subducted materials, followed by fractional crystallization.

There is no definitive evidence that plate tectonics ever operated on Mars, although recent studies of escarpments and compressional features in the TSC region around the Eridania basins have been interpreted as overthrust or an onset of subduction of hydrated terrains underneath a hanging wall [91]. If plate tectonics as we know it on Earth today did not occur on Mars, a pre-plate tectonic stage, similar to the tectonic regime observed in Archean terrains (4.0–2.5 Ga), might have started, enabling a hydrated basaltic crust to be partially melted and giving rise to evolved sub-alkaline compositions similar to those making up the Earth's continental crust. The hydrated melting of basaltic compositions could also occur without plate tectonics. A mantle plume could lead to partial melting of the lower part of a hydrated crust, or the existence of a thin lithosphere in the southern hemisphere would favor high temperatures in the lower/base of the crust resulting in the partial melting of it. The occurrence of sub-alkaline evolved rocks on Mars supports a hydrated crustal component in the southern hemisphere of Mars.

On Mars, the occurrence of water in the system is suggested by fractional and equilibrium crystallization models of various Martian basaltic compositions that present water to produce sub-alkaline melts [29,92] and the lack of sub-alkaline products in nominally anhydrous partial melting experiments of Martian primitive mantle compositions [86,93,94]. Most Martian meteorites do not have hydrous phases except for apatite grains and scarce amphibole in a few samples [95], but they are young (<2.4 Ga), originating from <15 ejection sites mainly located in the Tharsis province [3,61]. As mentioned in [96], the low water contents in the mantle estimated from Martian meteorites might thus be erroneous and be

the result of degassing, as well as sample bias. Note that the mineralogy of igneous rocks found in Gale crater was not directly analyzed, which prevents the identification of all the phases present in each rock. Inversion models considering Mars' thermal evolution show that the Martian mantle contained an average of 600 ppm in the Noachian period, which is close to terrestrial values today [97,98]. Such water amounts would be sufficient to form mantle-derived melts with $\text{H}_2\text{O} = 0.6 \text{ wt.}\%$, forming magmas with $>1 \text{ wt.}\%$ of H_2O during equilibrium or fractional crystallization processes.

3.2. Composition of the Ancient Martian Crust

All datasets currently available suggest the occurrence of evolved terrains in the ancient southern hemisphere, including in the TSC region that contains Gale crater and the possible ejection site of NWA 7533, both presenting evolved igneous materials. The *Insight* mission that landed on the Western side of Elysium Planitia in 2018 (Figure 3) analyzed the seismic activities of Mars, deducing crustal properties, including its density. Based on the first average crustal thickness ever calculated through seismic data, as well as gravity and topography data [33,99], the maximum density of the Martian crust was estimated between 2850 and 3100 $\text{kg}\cdot\text{m}^{-3}$. These values are consistent with previous estimations that solely used gravity and topography data (2700–3100 $\text{kg}\cdot\text{m}^{-3}$; [32,50]). Young mafic SNC, mafic rocks analyzed by *Spirit*, and mafic surface compositions measured by the Gamma Ray Spectrometer onboard the Mars Odyssey orbiter have a density higher than 3100 $\text{kg}\cdot\text{m}^{-3}$, suggesting that a buried light crustal component is needed to produce the lower densities estimated by geophysical and seismic data. Several authors [32,33,50] proposed the occurrence of an evolved crustal component beneath the dense mafic surface observed in young materials by orbiters. This is consistent with the CRISM detections of feldspar-bearing evolved terrains mainly exposed at the surface by impacts, erosion, and fractures, as well as with the discovery in Gale crater of intermediate and felsic rocks that likely originated from the rim or watershed northwest of Gale crater. NWA 7034 and its pairs are breccias formed through the lithification of impact debris consisting of various clasts and minerals embedded in a fine-grained matrix, suggesting that the Noachian igneous clasts are also excavated materials. The existence of a buried evolved crustal component below the mafic surface rather than several localized evolved outcrops within a mafic crust agrees with all datasets, explaining the relatively low-density component deduced from geophysical data.

Without a large compositional dataset and seismic data from various locations on Mars, depicting the exact composition of the Martian crust, including its alkaline or sub-alkaline nature and the relationship between feldspar-rich and LCP-rich terrains, is challenging. LCP and alkaline magmas are likely related by fractionation processes (Section 3.1), but the composition of feldspar-bearing terrains is unclear, preventing an understanding of the magmatic processes. The occurrence of sub-alkaline evolved rocks in Gale crater located in the Northwest region of TSC, the ejection site of NWA 7034 suggesting a 4.54 Ga enriched andesitic-like crust localized in the eastern TSC, and the multiple feldspar-rich evolved rocks detected in TSC support an intermediate to felsic crustal component of possible sub-alkaline compositions at that location.

Whether TSC is the remnant of a global evolved early crust is difficult to assess. Mars' crust could be heterogeneous with at least one relatively low-density evolved component at TSC, and, perhaps, additional locations where feldspar-bearing rocks of evolved compositions have been found on Mars (Figure 3). The presence of both LCP- and feldspar-rich rocks in the northern rim of the Hellas basin and within the Valles Marineris walls could be related to another complex crustal component with a dual mineralogy. This is in agreement with large impact basins like the Hellas basin, formed by impactors $> 100 \text{ km}$ in size, which could have partially melted the basement [100], forming an impact-induced layered formation with heavy minerals sinking (LCP) and light minerals floating (feldspar; [79]). The other scenario is a homogeneous evolved ancient crust in the southern hemisphere that was subsequently covered by mafic materials. The low crustal density calculated by

geophysical and seismic data suggest that the majority of that crust would be evolved. The low-Ca pyroxene observed within the cumulate meteorite ALH 84001 and within excavated ancient terrains would thus be minimal due to their high density ($>3400 \text{ kg}\cdot\text{m}^{-3}$ versus a maximum crustal density $<3100 \text{ kg}\cdot\text{m}^{-3}$).

3.3. Perspectives on Future Missions

Two main questions remain regarding the early Martian crust: (1) what is its exact petrology (e.g., mineralogy, evolved, sub-alkaline, or alkaline)? and (2) how did it form? Future missions are key to answering these unknowns, and this section aims to provide guidance for future missions that could unravel these questions. Table 1 summarizes the models for early Martian crust formation and the predicted crustal properties that would result from these scenarios. Table 2 summarizes the measurements and instruments that could characterize these properties during future missions to Mars.

3.3.1. Locations to Explore the Early Martian Crust

Both LCP and feldspar have been detected in exposed Noachian terrains (Figure 3), suggesting a possible bimodal Martian crust. Their petrology is yet uncertain due to the lack of centimeter- to millimeter-scale images, as well as chemical compositions and a complete mineralogy. The lithology of feldspar-rich regions differs depending on studies: anorthosites, granites, feldspar cumulates, feldspar-bearing basalts, felsic lava flows, and feldspar-rich evolved igneous rocks have all been proposed in regions where feldspar is detected from orbit [18–20,78–80,84]. The petrology of LCP terrains is also ambiguous, with dark-toned terrains possibly of mafic compositions (e.g., gabbroic or noritic), and white-toned terrains suggesting the possible occurrence of abundant feldspar [75].

In order to test the hypotheses of LCP being related to alkaline rocks and to better understand the petrology of these terrains, the potential relationship between LCP and feldspar, and the formation of such heterogeneous crust, future missions should investigate regions exhibiting excavated Noachian crust terrains where both LCP and feldspar have been detected with remote sensing (white and black starts in Figure 3). Deep impact craters, faults, and eroded terrains in Hellas basin, TSC, and Valles Marineris could be the targeted locations. Hellas basin is a 2300 km-diameter impact crater which is 6.5 km deep, exposing in its walls Early Noachian ($>3.9 \text{ Ga}$) igneous outcrops that exhibit LCP and feldspar spectral absorptions in CRISM datasets [73,75,79,80]. The TSC includes the ejection site of NWA 7034 (Figure 3), with detections of LCP and feldspar in different terrains in the vicinity, and exposes early Noachian crustal outcrops with possible compressional features. Valles Marineris, the largest and deepest canyon in the solar system, provides a profile of up to 7 km deep cutting through the crust, exposing Early Noachian outcrops also associated with LCP and feldspar absorptions in the lower part of the walls [73,80]. Hellas Basin walls, TSC, and walls of the Valles Marineris canyon are large regions with Noachian crustal exposures exhibiting both LCP and feldspar spectral signals. Exploring these regions would enable the characterization of textural and chemical variations of the crust through time (depth) and space (lateral).

3.3.2. Characterization of the Petrology of the Martian Crust

Characterizing the petrology of the Martian crust is crucial to constraining how it was formed and the localized, regional, or global scale of its formation, and igneous rocks are key to accessing this information, since the early crust is one of the products of magma ocean crystallization and subsequent magmatic processes [101]. Constraining the petrology of igneous rocks and their context enables us to not only depict the planet's magmatic evolution and mantle conditions such as pressure, oxygen fugacity, and water content, but also assess the scale of crust-forming events: localized versus regional to global magmatic processes. For instance, finding dioritic rocks in exposed ancient crustal exposures would likely indicate localized hydrous partial melting, while frequent diorites in these locations would rather suggest global hydrous partial melting. Trace elements and

isotopic analyses are then essential for inferring the specifics of igneous rock formation (e.g., the crystallization of mantle-derived melts versus the partial melting of a primary crust; Table 1).

Table 1. Hypotheses for formation of evolved Martian crust and possible properties.

	Model	Predicted Properties	
		Structure	Petrology
Primary evolved crust	Partial magma ocean	Heterogenous crust at a global scale with evolved and mafic components	Mafic rocks and evolved rocks with high Mg#; REE pattern relatively flat
	Crystallization of enriched component within global magma ocean		Igneous rocks rich in incompatible elements, i.e., K, P, and incompatible REE similar to lunar KREEP
Secondary evolved crust	Re-melting of a hydrated basaltic crust through hot melts extracted from a mantle plume, and fractional crystallization	Large- to global-scale evolved crust	Sub-alkaline calc-alkaline intermediate and felsic rocks with water-bearing minerals such as mica, amphibole, and OH-apatite. Possibly granitic/dioritic intrusions.
	Re-melting of an anhydrous basaltic crust through hot melts extracted from a mantle plume, and fractional crystallization		Alkaline intermediate and felsic rocks without hydrated minerals. Possibly monzonitic or alkali-granitic rocks. Possible LCP cumulates if fractional crystallization occurs.
	Re-melting of hydrated basaltic crust through tectonic processes (initiation of proto-plate tectonics) and fractional crystallization	- Regional patterns of intermediate to felsic domes surrounded by mafic terrains or vice versa - Potential patterns of paleomagnetism indicative of crustal spreading/subduction centers (requires Mars to have had alternating polarity)	Sub-alkaline evolved components including calc-alkaline rocks, granites, and granodiorites
	Re-melting of anhydrous basaltic crust through tectonic processes (initiation of proto-plate tectonics) and fractional crystallization	- Extension and compression faults associated with regional petrographic dome pattern or paleomagnetic patterns	Alkaline intermediate and felsic rocks. Possibly monzonitic or alkali-granitic rocks. Possible LCP cumulates if fractional crystallization occurs.
	Fractionation of impact melt	Depth profile showing a layered crust with phenocrystal texture	Mafic olivine and LCP cumulates/intrusions at the bottom and feldspar-rich rocks of evolved compositions at the top, similar to terrestrial impacts like the Sudbury crater (e.g., [102])
Mafic crust with localized evolved bodies	Mafic crust with local crystallization and/or partial melting processes	Plains of mafic rocks including at depth, with localized intrusions of intermediate and felsic rocks within a large depth profile and spatial range	Mafic composition and mineralogy (e.g., olivine, pyroxene, and plagioclase) at the surface and depth with non-continuous localized intermediate and felsic composition and mineralogy (e.g., feldspar-rich rocks, and quartz)

The petrology of the early crust can be constrained by coordinated imaging, mineral measurements, and the quantification of the major, minor, and trace elements in early Noachian igneous rocks. Similar to identifying the petrography of a terrestrial rock, centimeter- to micrometer-scale images will provide textural information. Mineralogical and chemical analyses will enable further rock classification. This information is critical to distinguishing between hypothesized models for crust formation, and made even more powerful when combined with kilometer-scale information about the crust structure and magnetic properties (Table 1).

A future mission capable of characterizing the petrology of the early Martian crust over a large region (>tens of km) would reveal the extent of evolved compositions, how texturally and compositionally diverse they are, and their relationship with possibly mafic ancient units, enabling an estimation of the bulk early Martian crust composition and its petrology. An orbiter would provide the greatest spatial coverage. Onboard, an imager with a spatial resolution similar to the HiRISE instrument onboard the Mars Reconnaissance orbiter could resolve features at ~1 m per pixel, although the phaneritic, porphyritic, or aphanitic texture of the igneous outcrop could not be observed [103]. Next-generation orbital VNIR imaging spectrometers (e.g., [104]) could characterize the mineralogy at a ~6 m scale and provide coupled high-resolution imaging at a scale of 10s of centimeters. A thermal imager of a <50 m spatial resolution similar to the Hayabusa 2 and OSIRIS-REX thermal emission spectrometers (e.g., [105,106]) would enable the quantitative characterization of the SiO₂ concentration of igneous terrains larger than the instrument's spatial resolution, distinguishing between mafic and evolved rocks, as well as providing information regarding the grain size of the materials based on their thermal inertia. However, orbital datasets are limited in that they cannot provide the centimeter to millimeter spatial resolution necessary to resolve the petrology. Elemental compositional measurements from orbit are also challenging with a gamma-ray spectrometer due to limitations in measuring all major elements like Na and Al concentrations and the kilometeric spatial resolution since the spatial resolution is proportional to the altitude of the spacecraft (300 km for the Gamma-Ray Spectrometer onboard Mars Odyssey).

In contrast, rovers enable chemical and mineralogical analyses at the petrologic scale (centimeter to micrometer) as illustrated by the *Curiosity* and *Perseverance* rovers. However, the coverage of these measurements is restricted to the travel capacity of a rover, i.e., a ~45 km total traversed to date with the *Opportunity* rover.

A third option of an aerial platform presents an attractive alternative because it could cover a larger spatial area than a rover while still enabling centimeter- to millimeter-scale compositional measurements. The *Ingenuity* helicopter on the Mars 2020 *Perseverance* mission proved the feasibility of flying on a planetary body with a very low atmospheric pressure. Looking forward, the Mars Science Helicopter concept [107] can carry up 5 kg of science payload, and could carry compositional instruments such as micro-LIBS coupled with an imager of micrometric spatial resolution [108] and a miniaturized imaging VNIR spectrometer [109]. Such a vessel could travel over large surfaces to measure the composition and mineralogy of various ancient outcrops representative of the early Martian crust in excavated regions. It would also enable us to precisely image and characterize contacts between evolved and mafic units, which would provide insights into the formation mechanism of the early Martian crust (Table 1). For instance, the relationship between LCP and feldspar outcrops are ambiguous, with either layer being on the top of each other or without clear contacts. Their co-occurrence in Noachian terrains yet suggest a possible bimodality of the ancient Martian crust. The lack of petrological information of LCP and feldspar outcrops thus prevents an understanding of the petrology and formation of the early crust. A helicopter detecting LCP and feldspar could document the possible contact with the high-resolution imager (μm scale), and decipher their petrology using micro-LIBS, allowing a better understanding of their formation.

3.3.3. Deciphering the Formation of an Evolved Martian Crust

Multiple scenarios have been suggested to explain the formation of an evolved crustal component [8,9,13,20,110,111]; but new measurements from current and future missions, as well as the Mars Sample Return mission, are now necessary in order to narrow down the most plausible scenario. Below are summarized the proposed formation mechanisms:

- An evolved primary crust; i.e., the first crust that was extracted from the magma ocean was evolved in composition and not basaltic. Several possibilities have been envisioned for this scenario (Figure 4A): (1) Cooling of a partial magma ocean, where relatively high degrees of partial melting (>20% of melting; [112,113]) of the chondritic planetesimals

would have led to intermediate and felsic sub-alkaline crustal compositions, as suggested by feldspar-rich andesitic achondrites [112,113]. The distinct D/H isotopic ratios in Martian meteorites, considered as primordial features of Mars' mantle, support a heterogeneous mantle that was poorly mixed during planetary accretion and differentiation [114]. The crystallization of a partial magma ocean is, thus, a possibility that should be envisioned in future differentiation models. (2) Another scenario considers that the crystallization of an enriched residual melt formed in late stages of the magma ocean could produce evolved compositions (Figure 4A; [20,110]).

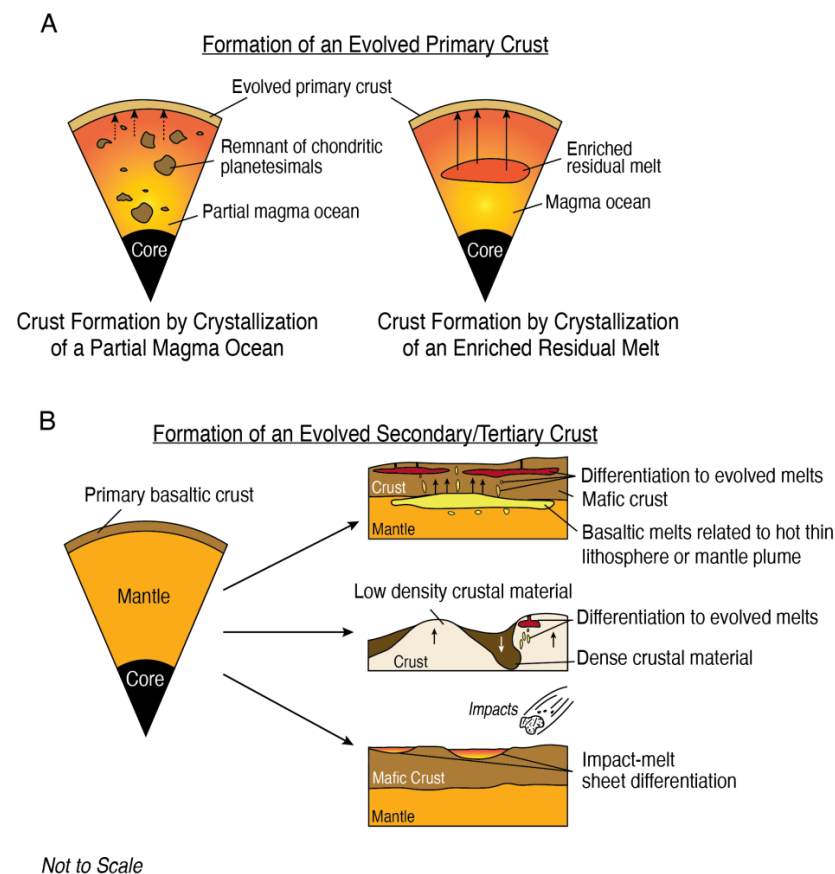


Figure 4. Illustrations simplifying the scenarios suggested in the literature to explain the formation of evolved crustal component(s) on Mars. **(A)** A primary evolved crust has been explained by a partial magma ocean where chondritic planetesimals did not all melt during accretion and various melting degrees of the chondritic components could explain the formation of evolved sub-alkaline compositions as proposed for the formation of andesitic achondrites [112,113]. The dashed arrows illustrate the extraction of the primary crust (left). An alternative is the occurrence of an enriched residual melt in late stage of the full magma ocean that would crystallize an evolved crustal component (right). **(B)** Scenarios of a secondary/tertiary evolved crust formed after the extraction from the magma ocean of a primary basaltic crust. (top right) Re-melting of the base of the crust by a mantle plume or high temperatures related to a thicker crust in the southern hemisphere compared to the northern lowlands would crystallize and differentiate to sub-alkaline evolved rocks representative of a secondary/tertiary evolved crustal component. (middle right) An example of an onset of plate tectonics possibly similar to proto-plate tectonics on Earth with Archean domes where dense mafic surface/upper crust would sink within the lithosphere, which would lead to partial melting of the mafic rocks and produce evolved sub-alkaline melts intruding the overlying crust. Lower-density materials would rise. (bottom right) Heavy bombardments early in Martian history would have led to impact melt sheets that would differentiate into layered bodies, with dense minerals (e.g., olivine and orthopyroxene) sinking at the bottom forming cumulates, and lighter phases (e.g., feldspar, and residual Si-rich glass) floating at the surface forming evolved upper layers.

- A secondary evolved crust, i.e., a crust formed after the modification of the primary crust, such as heavy volcanism and impact (Figure 4B). Three main possibilities can be envisioned, although a combination of the three is possible: (1) mantle-related, (2) tectonic-related, or (3) impact-related. (1) The re-melting of the base of a primary basaltic crust has been suggested through either a mantle plume extracting hot magmas [1] or a thick crust in the southern hemisphere that led to a thinner lithosphere and higher temperatures, and, thus, partial melting and differentiation processes at the base of the crust, in agreement with thermal evolution models using seismic constraints from the InSight lander [111]. The presence of water would facilitate the formation of intermediate and felsic melts as observed on Earth [70], which is expected to be the case according to inversion thermal models estimating up to 600 ppm in the Martian mantle in Noachian time [97]. (2) Another scenario for a secondary/tertiary evolved crust is an onset of plate tectonics potentially similar to the Archean stage. The overthrust of large regions on the Eridania basin terrains have been suggested as a signature of crustal recycling with lithospheric delamination, possibly similar to pre-plate tectonic features on Earth [115]. (3) A final hypothesis is the formation of an evolved crust through intense large impacts. Impactors of a >100 km diameter produce crustal and mantle melts, which could differentiate to evolved compositions [100,116]. In all the scenarios, the re-melting of a basaltic crust possibly followed by fractional crystallization would form sub-alkaline melts, likely leading to an evolved sub-alkaline crust.

In order to decipher the formation mechanism of a complex crust on Mars, both regional imaging that could show the extent of evolved rocks and their relationship to possible mafic surroundings, as well as isotopic and trace element compositional analyses are crucial. Table 2 summarizes a non-exhaustive list of observations and measurements that would help to back out the formation of a complex early crust on Mars.

Table 2. Type of measurements needed from orbiting and in situ Martian missions for understanding the nature of the early Martian crust.

Objectives	Analyses	Possible Instrumentation	Platform
Constraining the elemental composition of the crust	Major, minor, and trace element analyses, including rare earth element	- Laser-Induced Breakdown Spectroscopy (LIBS) for major and trace elements (Rb, Sr, Ba, Cr, Ni, La, Ce, Eu, Gd, Dy, Nd, Pr, Sm, Y) - X-ray Fluorescence (XRF) - Alpha Particle X-ray Spectrometer (APXS)	Rover, lander, helicopter
Constraining the petrology of the crust	High-resolution images	Color images of ~15 µm/pixel imaging: MAHLI resolution	Rover, lander, helicopter
	Chemical measurement of single minerals	LIBS at micron scale to analyze the composition of single phenocrysts	Rover, lander, helicopter
	Mineralogy	- Bulk X-ray Diffraction (XRD) Raman VSWIR at m to mm resolution TIR at m to mm resolution	Rover or lander, helicopter, orbiter
Constraining the physical properties of the crust and possible onset of tectonics	Regional imaging	Color images with mm to cm resolution	Helicopter or orbiter
	Regional paleomagnetism	Low-altitude magnetic measurements [117]	Helicopter or orbiter
	Regional mineralogy	Meter- to centimeter-scale VSWIR and TIR spectral datasets	Helicopter or orbiter
	Regional structure	Seismometers, gravimeter	Lander, helicopter

Questions regarding whether an onset of plate tectonics did start on Mars and is the cause of an evolved crustal component could be answered by high-resolution regional imaging similar to current resolutions (e.g., HiRISE and CTX) to search for any thrust and extension faults, as well as possible circular patterns with domes similar to the Archean crust (Figure 4B). A helicopter or low-orbit spacecraft could provide such information, and onboard instrumentation enabling chemical and mineralogical analyses (e.g., LIBS, XRF, and VNIR spectroscopy) would be important for comparisons with Archean crustal residues.

On Earth, understanding the formation of the early crust is a challenge due to the lack of samples (~3% of the exposed continental crust is Archean, i.e., 4.0–2.5 Ga) and weathering, but the availability of trace element concentrations and isotopic analyses of Archean igneous rocks is imperative to rule out some formation processes and refine others (e.g., [118]). Isotopic and REE analyses are of significance to eliminate scenarios, but most of these measurements require heavy sample preparation including dissolution, leaching, rinsing, and drying procedures that are challenging for a remotely controlled payload. The Mars Sample Return (MSR) mission is thus essential for obtaining trace element and isotopic analyses of Early Noachian igneous samples in Earth-based labs with mass spectrometers. Some chemical analyses onboard a ground mission could also provide valuable insights into the formation mechanisms of an evolved crustal component. Several light and heavy trace elements can be analyzed by miniaturized instruments already existing onboard rovers like LIBS and APXS (e.g., Rb, Sr, Ba, Cr, Ni, La, Ce, Eu, Gd, Dy, Nd, Pr, Sm, and Y). These elements can provide first insights into the depleted/enriched nature of the magmatic reservoir, as well as the presence of one or several reservoirs which evolved rocks originated from. Such information is essential for understanding the magmatic processes involved in the generation of an evolved crustal component.

4. Conclusions

Martian meteorites, rover, and orbital measurements demonstrated the occurrence of alkaline and sub-alkaline mafic and evolved rocks and outcrops from the Noachian period. The extents and relationships between mafic and evolved regions are yet uncertain, preventing an understanding of the petrology of the early Martian crust. Two magmatic suites were observed in Gale crater by the *Curiosity* rover, with a sub-alkaline and an alkaline series, suggesting that they formed in different ways. On Earth, alkaline magmas can be formed through melting of a metasomatized mantle, high-pressure partial melting, or fractional crystallization combined with crustal assimilation, while sub-alkaline melts are related to re-melting of mafic materials or fractionation of mafic melts. A possible andesitic crust extracted as early as 20 Myr after the solar system formation and >3.7 Ga diorites in Gale crater could indicate a sub-alkaline evolved crust in the southern hemisphere, suggesting re-melting of basaltic materials or fractionation of basaltic melts. The primary or secondary/tertiary nature of such an evolved crust and its formation mechanism cannot be asserted without additional chemical and mineralogical information of Noachian evolved igneous outcrops. The evolved crustal component(s) below a mafic surface are supported by geophysical and seismic data, but characterizing its mineralogy and composition is crucial in order to constrain its formation mechanisms. The Terra Sirenum/Cimmeria region includes: (1) where evolved Noachian igneous rocks were found in Gale crater, (2) where the ejection site of NWA 7034 and its pairs has been located, and (3) excavated feldspar-rich evolved regions which have been observed with CRISM, suggesting that TSC could be an evolved crustal remnant. Future Martian missions are essential for deciphering the simple question of what the petrology of the Martian crust is. The Mars Sample Return (MSR) and a helicopter mission would be fundamental for measuring trace element compositions, which would provide powerful insights into the formation of the early Martian crust and resolve the enigmatic nature of the Martian crust. The composition of Mars' crust has relevance on astrobiology aspects as well, since an evolved crust would likely contain lithophile elements influencing prebiotic processes [119].

Author Contributions: Conceptualization, V.P.; methodology, V.P., A.U. and A.A.F.; validation, V.P., A.U. and A.A.F.; investigation, V.P., A.U. and A.A.F.; resources, V.P., A.U. and A.A.F.; writing—original draft preparation, V.P., A.U. and A.A.F.; writing—review and editing, V.P., A.U. and A.A.F.; visualization, V.P. and A.U. All authors have read and agreed to the published version of the manuscript.

Funding: This research received no external funding.

Data Availability Statement: All the data presented in this paper are available in publications and in the Planetary Data System (<https://pds-geosciences.wustl.edu/>).

Acknowledgments: We are grateful for Violaine Sautter’s inputs and feedbacks in the organization and content of the article. We are thankful to the reviewers and editors for their insightful comments that improved the manuscript. A portion of this research was carried out at the Jet Propulsion Laboratory, California Institute of Technology, under a contract with the National Aeronautics and Space Administration (80NM0018D0004).

Conflicts of Interest: The authors declare no conflicts of interest.

References

- Sautter, V.; Toplis, M.J.; Beck, P.; Mangold, N.; Wiens, R.; Pinet, P.; Cousin, A.; Maurice, S.; LeDeit, L.; Hewins, R.; et al. Magmatic Complexity on Early Mars as Seen through a Combination of Orbital, in-Situ and Meteorite Data. *Lithos* **2016**, *254–255*, 36–52. [[CrossRef](#)]
- Changela, H.G.; Chatzitheodoridis, E.; Antunes, A.; Beaty, D.; Bouw, K.; Bridges, J.C.; Capova, K.A.; Cockell, C.S.; Conley, C.A.; Dadachova, E.; et al. Mars: New Insights and Unresolved Questions. *Int. J. Astrobiol.* **2021**, *20*, 394–426. [[CrossRef](#)]
- Udry, A.; Howarth, G.H.; Herd, C.D.K.; Day, J.M.D.; Lapen, T.J.; Filiberto, J. What Martian Meteorites Reveal about the Interior and Surface of Mars. *J. Geophys. Res. Planets* **2020**, *125*, e2020JE006523. [[CrossRef](#)]
- Collinet, M.; Plesa, A.-C.; Ruedas, T.; Schwinger, S.; Breuer, D. The Temperature and Composition of the Mantle Sources of Martian Basalts. *Geophys. Res. Lett.* **2023**, *50*, e2023GL103537. [[CrossRef](#)]
- Gyollai, I.; Chatzitheodoridis, E.; Kereszturi, Á.; Szabó, M. Multiple Generation Magmatic and Hydrothermal Processes in a Martian Subvolcanic Environment Based on the Analysis of Yamato-000593 Nakhlite Meteorite. *Meteorit. Planet. Sci.* **2023**, *58*, 218–240. [[CrossRef](#)]
- Aucamp, T.; Howarth, G.H.; Peel, C.J.; Costin, G.; Day, J.M.D.; le Roux, P.; Scott, J.M.; Greshake, A.; Bartoschewitz, R. Petrogenesis of the Dar al Gani (DaG) 1.1 Ma Ejection-Paired Olivine-Phyric Shergottites and Implications for 470 Ma Martian Volcanism. *Meteorit. Planet. Sci.* **2023**, *58*, 1654–1676. [[CrossRef](#)]
- Jennings, E.S.; Coull, P. Olivine Microstructure and Thermometry in Olivine-Phyric Shergottites Sayh al Uhaymir 005 and Dar al Gani 476. *Meteorit. Planet. Sci.* **2024**, *59*, 55–67. [[CrossRef](#)]
- Bouvier, L.C.; Costa, M.M.; Connelly, J.N.; Jensen, N.K.; Wielandt, D.; Storey, M.; Nemchin, A.A.; Whitehouse, M.J.; Snape, J.F.; Bellucci, J.J.; et al. Evidence for Extremely Rapid Magma Ocean Crystallization and Crust Formation on Mars. *Nature* **2018**, *558*, 586. [[CrossRef](#)] [[PubMed](#)]
- Humayun, M.; Nemchin, A.; Zanda, B.; Hewins, R.H.; Grange, M.; Kennedy, A.; Lorand, J.-P.; Göpel, C.; Fieni, C.; Pont, S.; et al. Origin and Age of the Earliest Martian Crust from Meteorite NWA 7533. *Nature* **2013**, *503*, 513–516. [[CrossRef](#)]
- Hewins, R.H.; Zanda, B.; Humayun, M.; Nemchin, A.; Lorand, J.-P.; Pont, S.; Deldicque, D.; Bellucci, J.J.; Beck, P.; Leroux, H.; et al. Regolith Breccia Northwest Africa 7533: Mineralogy and Petrology with Implications for Early Mars. *Meteorit. Planet. Sci.* **2017**, *52*, 89–124. [[CrossRef](#)]
- Santos, A.R.; Agee, C.B.; McCubbin, F.M.; Shearer, C.K.; Burger, P.V.; Tartèse, R.; Anand, M. Petrology of Igneous Clasts in Northwest Africa 7034: Implications for the Petrologic Diversity of the Martian Crust. *Geochim. Cosmochim. Acta* **2015**, *157*, 56–85. [[CrossRef](#)]
- Wittmann, A.; Korotev, R.L.; Jolliff, B.L.; Irving, A.J.; Moser, D.E.; Barker, I.; Rumble, D. Petrography and Composition of Martian Regolith Breccia Meteorite Northwest Africa 7475. *Meteorit. Planet. Sci.* **2015**, *50*, 326–352. [[CrossRef](#)]
- Sautter, V.; Toplis, M.J.; Wiens, R.C.; Cousin, A.; Fabre, C.; Gasnault, O.; Maurice, S.; Forni, O.; Lasue, J.; Ollila, A.; et al. In Situ Evidence for Continental Crust on Early Mars. *Nat. Geosci.* **2015**, *8*, 605–609. [[CrossRef](#)]
- Cousin, A.; Sautter, V.; Payré, V.; Forni, O.; Mangold, N.; Gasnault, O.; Le Deit, L.; Johnson, J.; Maurice, S.; Salvatore, M.; et al. Classification of Igneous Rocks Analyzed by ChemCam at Gale Crater, Mars. *Icarus* **2017**, *288*, 265–283. [[CrossRef](#)]
- Sautter, V.; Payré, V. Alkali Magmatism on Mars: An Unexpected Diversity. *Comptes Rendus Géosci.* **2021**, *353*, 61–90. [[CrossRef](#)]
- Christensen, P.R.; Bandfield, J.L.; Smith, M.D.; Hamilton, V.E.; Clark, R.N. Identification of a Basaltic Component on the Martian Surface from Thermal Emission Spectrometer Data. *J. Geophys. Res. Planets* **2000**, *105*, 9609–9621. [[CrossRef](#)]
- Ehlmann, B.L.; Edwards, C.S. Mineralogy of the Martian Surface. *Annu. Rev. Earth Planet. Sci.* **2014**, *42*, 291–315. [[CrossRef](#)]
- Rogers, A.D.; Farrand, W.H. Spectral Evidence for Alkaline Rocks and Compositional Diversity among Feldspathic Light-Toned Terrains on Mars. *Icarus* **2022**, *376*, 114883. [[CrossRef](#)]
- Wray, J.J.; Hansen, S.T.; Dufek, J.; Swayze, G.A.; Murchie, S.L.; Seelos, F.P.; Skok, J.R.; Irwin, R.P.; Ghiorso, M.S. Prolonged Magmatic Activity on Mars Inferred from the Detection of Felsic Rocks. *Nat. Geosci.* **2013**, *6*, 1013–1017. [[CrossRef](#)]

20. Payré, V.; Salvatore, M.R.; Edwards, C.S. An Evolved Early Crust Exposed on Mars Revealed Through Spectroscopy. *Geophys. Res. Lett.* **2022**, *49*, e2022GL099639. [[CrossRef](#)]
21. McSween, H.Y.; Ruff, S.W.; Morris, R.V.; Bell, J.F.; Herkenhoff, K.; Gellert, R.; Stockstill, K.R.; Tornabene, L.L.; Squyres, S.W.; Crisp, J.A.; et al. Alkaline Volcanic Rocks from the Columbia Hills, Gusev Crater, Mars. *J. Geophys. Res.* **2006**, *111*, E09S91. [[CrossRef](#)]
22. McSween, H.Y.; Wyatt, M.B.; Gellert, R.; Bell, J.F.; Morris, R.V.; Herkenhoff, K.E.; Crumpler, L.S.; Milam, K.A.; Stockstill, K.R.; Tornabene, L.L.; et al. Characterization and Petrologic Interpretation of Olivine-Rich Basalts at Gusev Crater, Mars. *J. Geophys. Res. Planets* **2006**, *111*, E02S10. [[CrossRef](#)]
23. Udry, A.; Ostwald, A.; Sautter, V.; Cousin, A.; Beyssac, O.; Forni, O.; Dromart, G.; Benzerara, K.; Nachon, M.; Horgan, B.; et al. A Mars 2020 Perseverance SuperCam Perspective on the Igneous Nature of the Máaz Formation at Jezero Crater and Link with Séítah, Mars. *J. Geophys. Res. Planets* **2022**, *128*, e2022JE007440. [[CrossRef](#)]
24. Wiens, R.C.; Udry, A.; Beyssac, O.; Quantin-Nataf, C.; Mangold, N.; Cousin, A.; Mandon, L.; Bosak, T.; Forni, O.; McLennan, S.M.; et al. Compositionally and Density Stratified Igneous Terrain in Jezero Crater, Mars. *Sci. Adv.* **2022**, *8*, eabo3399. [[CrossRef](#)] [[PubMed](#)]
25. McSween, H.Y.; Taylor, G.J.; Wyatt, M.B. Elemental Composition of the Martian Crust. *Science* **2009**, *324*, 736–739. [[CrossRef](#)] [[PubMed](#)]
26. Ramsey, M.S.; Christensen, P.R. Mineral Abundance Determination: Quantitative Deconvolution of Thermal Emission Spectra. *J. Geophys. Res. Solid Earth* **1998**, *103*, 577–596. [[CrossRef](#)]
27. Rudnick, R.L.; Gao, S. Composition of the Continental Crust. In *Treatise on Geochemistry*; Elsevier: Amsterdam, The Netherlands, 2003; pp. 1–64, ISBN 978-0-08-043751-4.
28. Irvine, T.N.; Baragar, W.R.A. A Guide to the Chemical Classification of the Common Volcanic Rocks. *Can. J. Earth Sci.* **1971**, *8*, 523–548. [[CrossRef](#)]
29. Udry, A.; Gazel, E.; McSween, H.Y. Formation of Evolved Rocks at Gale Crater by Crystal Fractionation and Implications for Mars Crustal Composition. *J. Geophys. Res. Planets* **2018**, *123*, 1525–1540. [[CrossRef](#)]
30. Payré, V.; Siebach, K.L.; Dasgupta, R.; Udry, A.; Rampe, E.B.; Morrison, S.M. Constraining Ancient Magmatic Evolution on Mars Using Crystal Chemistry of Detrital Igneous Minerals in the Sedimentary Bradbury Group, Gale Crater, Mars. *J. Geophys. Res. Planets* **2020**, *125*, e2020JE006467. [[CrossRef](#)]
31. Ostwald, A.; Udry, A.; Payré, V.; Gazel, E.; Wu, P. The Role of Assimilation and Fractional Crystallization in the Evolution of the Mars Crust. *Earth Planet. Sci. Lett.* **2022**, *585*, 117514. [[CrossRef](#)]
32. Wieczorek, M.A.; Zuber, M.T. Thickness of the Martian Crust: Improved Constraints from Geoid-to-Topography Ratios. *J. Geophys. Res. Planets* **2004**, *109*, E01009. [[CrossRef](#)]
33. Wieczorek, M.A.; Broquet, A.; McLennan, S.M.; Rivoldini, A.; Golombek, M.; Antonangeli, D.; Beghein, C.; Giardini, D.; Gudkova, T.; Gyalay, S.; et al. InSight Constraints on the Global Character of the Martian Crust. *J. Geophys. Res. Planets* **2022**, *127*, e2022JE007298. [[CrossRef](#)]
34. Deng, S.; Levander, A. Autocorrelation Reflectivity of Mars. *Geophys. Res. Lett.* **2020**, *47*, e2020GL089630. [[CrossRef](#)]
35. Bouley, S.; Keane, J.T.; Baratoux, D.; Langlais, B.; Matsuyama, I.; Costard, F.; Hewins, R.; Payré, V.; Sautter, V.; Séjourné, A.; et al. A Thick Crustal Block Revealed by Reconstructions of Early Mars Highlands. *Nat. Geosci.* **2020**, *13*, 105–109. [[CrossRef](#)]
36. Lagain, A.; Bouley, S.; Zanda, B.; Miljković, K.; Rajšić, A.; Baratoux, D.; Payré, V.; Doucet, L.S.; Timms, N.E.; Hewins, R.; et al. Early Crustal Processes Revealed by the Ejection Site of the Oldest Martian Meteorite. *Nat. Commun.* **2022**, *13*, 3782. [[CrossRef](#)]
37. Lapen, T.J.; Richter, M.; Brandon, A.D.; Debaille, V.; Beard, B.L.; Shafer, J.T.; Peslier, A.H. A Younger Age for ALH84001 and Its Geochemical Link to Shergottite Sources in Mars. *Science* **2010**, *328*, 347–351. [[CrossRef](#)] [[PubMed](#)]
38. Mittlefehldt, D.W. ALH84001, a Cumulate Orthopyroxenite Member of the Martian Meteorite Clan. *Meteoritics* **1994**, *29*, 214–221. [[CrossRef](#)]
39. Treiman, A.H. A Petrographic History of Martian Meteorite ALH84001: Two Shocks and an Ancient Age. *Meteoritics* **1995**, *30*, 294–302. [[CrossRef](#)]
40. Kring, D.A.; Gleason, J.D. Magmatic Temperatures and Compositions on Early Mars as Inferred from the Orthopyroxene-Silica Assemblage in Allan Hills 84001. *Meteorit. Planet. Sci. Suppl.* **1997**, *32*, A74.
41. McKay, D.S.; Gibson, E.K.; Thomas-Keppta, K.L.; Vali, H.; Romanek, C.S.; Clemett, S.J.; Chillier, X.D.F.; Maechling, C.R.; Zare, R.N. Search for Past Life on Mars: Possible Relic Biogenic Activity in Martian Meteorite ALH84001. *Science* **1996**, *273*, 924–930. [[CrossRef](#)]
42. Treiman, A.H. Meteorite Allan Hills (ALH) 84001: Implications for Mars' Inhabitation and Habitability. *First Billion Years Habitability* **2019**, *2134*, 1032.
43. Kruijjer, T.S.; Kleine, T.; Borg, L.E.; Brennecka, G.A.; Irving, A.J.; Bischoff, A.; Agee, C.B. The Early Differentiation of Mars Inferred from Hf–W Chronometry. *Earth Planet. Sci. Lett.* **2017**, *474*, 345–354. [[CrossRef](#)]
44. Cannon, K.M.; Mustard, J.F.; Agee, C.B. Evidence for a Widespread Basaltic Breccia Component in the Martian Low-Albedo Regions from the Reflectance Spectrum of Northwest Africa 7034. *Icarus* **2015**, *252*, 150–153. [[CrossRef](#)]
45. Agee, C.B.; Wilson, N.V.; McCubbin, F.M.; Ziegler, K.; Polyak, V.J.; Sharp, Z.D.; Asmerom, Y.; Nunn, M.H.; Shaheen, R.; Thiemens, M.H.; et al. Unique Meteorite from Early Amazonian Mars: Water-Rich Basaltic Breccia Northwest Africa 7034. *Science* **2013**, *339*, 780–785. [[CrossRef](#)] [[PubMed](#)]

46. McCubbin, F.M.; Boyce, J.W.; Novak-Szabo, T.; Santos, A.; Tartese, R.; Muttik, N.; Domokos, G.; Vazquez, J.A.; Keller, L.P.; Moser, D.E.; et al. Geologic History of Martian Regolith Breccia Northwest Africa 7034: Evidence for Hydrothermal Activity and Lithologic Diversity in the Martian Crust. *J. Geophys. Res. E Planets* **2016**, *121*, 21202149. [[CrossRef](#)]
47. MacArthur, J.L.; Bridges, J.C.; Hicks, L.J.; Burgess, R.; Joy, K.H.; Branney, M.J.; Hansford, G.M.; Baker, S.H.; Schwenzer, S.P.; Gurman, S.J.; et al. Mineralogical Constraints on the Thermal History of Martian Regolith Breccia Northwest Africa 8114. *Geochim. Cosmochim. Acta* **2019**, *246*, 267–298. [[CrossRef](#)]
48. Leroux, H.; Jacob, D.; Marinova, M.; Hewins, R.H.; Zanda, B.; Pont, S.; Lorand, J.-P.; Humayun, M. Exsolution and Shock Microstructures of Igneous Pyroxene Clasts in the Northwest Africa 7533 Martian Meteorite. *Meteorit. Planet. Sci.* **2016**, *51*, 932–945. [[CrossRef](#)]
49. Udry, A.; Lunning, N.G.; McSween, H.Y.; Bodnar, R.J. Petrogenesis of a Vitrophyre in the Martian Meteorite Breccia NWA 7034. *Geochim. Cosmochim. Acta* **2014**, *141*, 281–293. [[CrossRef](#)]
50. Baratoux, D.; Samuel, H.; Michaut, C.; Toplis, M.J.; Monnereau, M.; Wiczorek, M.; Garcia, R.; Kurita, K. Petrological Constraints on the Density of the Martian Crust. *J. Geophys. Res. Planets* **2014**, *119*, 1707–1727. [[CrossRef](#)]
51. Filiberto, J.; Gross, J.; Trela, J.; Ferré, E.C. Gabbroic Shergottite Northwest Africa 6963: An Intrusive Sample of Mars. *Am. Mineral.* **2014**, *99*, 601–606. [[CrossRef](#)]
52. Lindner, M.; Hezel, D.C.; Gerdes, A.; Marschall, H.R.; Brenker, F.E. Young Magmatism and Si-Rich Melts on Mars as Documented in the Enriched Gabbroic Shergottite NWA 6963. *Meteorit. Planet. Sci.* **2022**, *57*, 2017–2041. [[CrossRef](#)]
53. Goderis, S.; Brandon, A.D.; Mayer, B.; Humayun, M. Ancient Impactor Components Preserved and Reworked in Martian Regolith Breccia Northwest Africa 7034. *Geochim. Cosmochim. Acta* **2016**, *191*, 203–215. [[CrossRef](#)]
54. Costa, M.M.; Jensen, N.K.; Bouvier, L.C.; Connelly, J.N.; Mikouchi, T.; Horstwood, M.S.A.; Suuronen, J.-P.; Moynier, F.; Deng, Z.; Agranier, A.; et al. The Internal Structure and Geodynamics of Mars Inferred from a 4.2-Gyr Zircon Record. *PNAS* **2020**, *117*, 30973–30979. [[CrossRef](#)] [[PubMed](#)]
55. Hu, S.; Lin, Y.; Zhang, J.; Hao, J.; Xing, W.; Zhang, T.; Yang, W.; Changela, H. Ancient Geologic Events on Mars Revealed by Zircons and Apatites from the Martian Regolith Breccia NWA 7034. *Meteorit. Planet. Sci.* **2019**, *54*, 850–879. [[CrossRef](#)]
56. Nyquist, L.E.; Shih, C.-Y.; McCubbin, F.M.; Santos, A.R.; Shearer, C.K.; Peng, Z.X.; Burger, P.V.; Agee, C.B. Rb-Sr and Sm-Nd Isotopic and REE Studies of Igneous Components in the Bulk Matrix Domain of Martian Breccia Northwest Africa 7034. *Meteorit. Planet. Sci.* **2016**, *51*, 483–498. [[CrossRef](#)]
57. Armytage, R.M.G.; Debaille, V.; Brandon, A.D.; Agee, C.B. A Complex History of Silicate Differentiation of Mars from Nd and Hf Isotopes in Crustal Breccia NWA 7034. *Earth Planet. Sci. Lett.* **2018**, *502*, 274–283. [[CrossRef](#)]
58. Amelin, Y.; Krot, A.N.; Hutcheon, I.D.; Ulyanov, A.A. Lead Isotopic Ages of Chondrules and Calcium-Aluminum-Rich Inclusions. *Science* **2002**, *297*, 1678–1683. [[CrossRef](#)] [[PubMed](#)]
59. Cassata, W.S.; Cohen, B.E.; Mark, D.F.; Trappitsch, R.; Crow, C.A.; Wimpenny, J.; Lee, M.R.; Smith, C.L. Chronology of Martian Breccia NWA 7034 and the Formation of the Martian Crustal Dichotomy. *Sci. Adv.* **2018**, *4*, eaap8306. [[CrossRef](#)] [[PubMed](#)]
60. Lapen, T.J.; Righter, M.; Andreasen, R.; Irving, A.J.; Satkoski, A.M.; Beard, B.L.; Nishiizumi, K.; Jull, A.J.T.; Caffee, M.W. Two Billion Years of Magmatism Recorded from a Single Mars Meteorite Ejection Site. *Sci. Adv.* **2017**, *3*, e1600922. [[CrossRef](#)]
61. Lagain, A.; Benedix, G.K.; Servis, K.; Baratoux, D.; Doucet, L.S.; Rajšić, A.; Devillepoix, H.A.R.; Bland, P.A.; Towner, M.C.; Sansom, E.K.; et al. The Tharsis Mantle Source of Depleted Shergottites Revealed by 90 Million Impact Craters. *Nat. Commun.* **2021**, *12*, 6352. [[CrossRef](#)]
62. McCoy, T.J.; Sims, M.; Schmidt, M.E.; Edwards, L.; Tornabene, L.L.; Crumpler, L.S.; Cohen, B.A.; Soderblom, L.A.; Blaney, D.L.; Squyres, S.W.; et al. Structure, Stratigraphy, and Origin of Husband Hill, Columbia Hills, Gusev Crater, Mars. *J. Geophys. Res. Planets* **2008**, *113*, E06S03. [[CrossRef](#)]
63. Arvidson, R.E.; Squyres, S.W.; Anderson, R.C.; Bell, J.F.; Blaney, D.; Brückner, J.; Cabrol, N.A.; Calvin, W.M.; Carr, M.H.; Christensen, P.R.; et al. Overview of the Spirit Mars Exploration Rover Mission to Gusev Crater: Landing Site to Backstay Rock in the Columbia Hills. *J. Geophys. Res.* **2006**, *111*, E02S01. [[CrossRef](#)]
64. Le Deit, L.; Hauber, E.; Fueten, F.; Pondrelli, M.; Rossi, A.P.; Jaumann, R. Sequence of Infilling Events in Gale Crater, Mars: Results from Morphology, Stratigraphy, and Mineralogy. *J. Geophys. Res. Planets* **2013**, *118*, 2439–2473. [[CrossRef](#)]
65. Farley, K.A.; Malespin, C.; Mahaffy, P.; Grotzinger, J.P.; Vasconcelos, P.M.; Milliken, R.E.; Malin, M.; Edgett, K.S.; Pavlov, A.A.; Hurowitz, J.A.; et al. In Situ Radiometric and Exposure Age Dating of the Martian Surface. *Science* **2014**, *343*, 1247166. [[CrossRef](#)] [[PubMed](#)]
66. Bowden, D.L.; Bridges, J.C.; Cousin, A.; Rapin, W.; Semprich, J.; Gasnault, O.; Forni, O.; Gasda, P.; Das, D.; Payré, V.; et al. Askival: An Altered Feldspathic Cumulate Sample in Gale Crater. *Meteorit. Planet. Sci.* **2023**, *58*, 41–62. [[CrossRef](#)]
67. Ehlmann, B.L.; Buz, J. Mineralogy and Fluvial History of the Watersheds of Gale, Knobel, and Sharp Craters: A Regional Context for the Mars Science Laboratory Curiosity's Exploration. *Geophys. Res. Lett.* **2015**, *42*, 264–273. [[CrossRef](#)]
68. Buz, J.; Ehlmann, B.L.; Pan, L.; Grotzinger, J.P. Mineralogy and Stratigraphy of the Gale Crater Rim, Wall, and Floor Units. *J. Geophys. Res. Planets* **2017**, *122*, 1090–1118. [[CrossRef](#)]
69. Filiberto, J. Geochemistry of Martian Basalts with Constraints on Magma Genesis. *Chem. Geol.* **2017**, *466*, 1–14. [[CrossRef](#)]
70. Rudnick, R.L. Making Continental Crust. *Nature* **1995**, *378*, 571–578. [[CrossRef](#)]
71. Mustard, J.F.; Poulet, F.; Gendrin, A.; Bibring, J.-P.; Langevin, Y.; Gondet, B.; Mangold, N.; Bellucci, G.; Altieri, F. Olivine and Pyroxene Diversity in the Crust of Mars. *Science* **2005**, *307*, 1594–1597. [[CrossRef](#)]

72. Poulet, F.; Mangold, N.; Platevoet, B.; Bardintzeff, J.-M.; Sautter, V.; Mustard, J.F.; Bibring, J.-P.; Pinet, P.; Langevin, Y.; Gondet, B.; et al. Quantitative Compositional Analysis of Martian Mafic Regions Using the MEx/OMEGA Reflectance Data: 2. Petrological Implications. *Icarus* **2009**, *201*, 84–101. [[CrossRef](#)]
73. Flahaut, J.; Quantin, C.; Clenet, H.; Allemand, P.; Mustard, J.F.; Thomas, P. Pristine Noachian Crust and Key Geologic Transitions in the Lower Walls of Valles Marineris: Insights into Early Igneous Processes on Mars. *Icarus* **2012**, *221*, 420–435. [[CrossRef](#)]
74. Brustel, C.; Flahaut, J.; Hauber, E.; Fueten, F.; Quantin, C.; Stesky, R.; Davies, G.R. Valles Marineris Tectonic and Volcanic History Inferred from Dikes in Eastern Coprates Chasma. *J. Geophys. Res. Planets* **2017**, *122*, 1353–1371. [[CrossRef](#)]
75. Brustel, C.P.A. Early Magmatic Processes on Mars. Ph.D. Thesis, Vrije Universiteit Amsterdam, Amsterdam, The Netherlands, 2021.
76. Baratoux, D.; Toplis, M.J.; Monnereau, M.; Sautter, V. The Petrological Expression of Early Mars Volcanism. *J. Geophys. Res. Planets* **2013**, *118*, 59–64. [[CrossRef](#)]
77. Tanaka, K.L.; Robbins, S.J.; Fortezzo, C.M.; Skinner, J.A.; Hare, T.M. The Digital Global Geologic Map of Mars: Chronostratigraphic Ages, Topographic and Crater Morphologic Characteristics, and Updated Resurfacing History. *Planet. Space Sci.* **2014**, *95*, 11–24. [[CrossRef](#)]
78. Carter, J.; Poulet, F. Ancient Plutonic Processes on Mars Inferred from the Detection of Possible Anorthositic Terrains. *Nat. Geosci.* **2013**, *6*, 1008–1012. [[CrossRef](#)]
79. Phillips, M.S.; Viviano, C.E.; Moersch, J.E.; Rogers, A.D.; McSween, H.Y.; Seelos, F.P. Extensive and Ancient Feldspathic Crust Detected across North Hellas Rim, Mars: Possible Implications for Primary Crust Formation. *Geology* **2022**, *50*, 1182–1186. [[CrossRef](#)]
80. Flahaut, J.; Payet, V.; Fueten, F.; Guitreau, M.; Barthez, M.; Ito, G.; Allemand, P. New Detections of Feldspar-Bearing Volcanic Rocks in the Walls of Valles Marineris, Mars. *Geophys. Res. Lett.* **2023**, *50*, e2022GL100772. [[CrossRef](#)]
81. Barthez, M.; Flahaut, J.; Guitreau, M.; Ito, G.; Pik, R. Understanding VNIR Plagioclase Signatures on Mars Through Petrographic, Geochemical, and Spectral Characterization of Terrestrial Feldspar-Bearing Igneous Rocks. *J. Geophys. Res. Planets* **2023**, *128*, e2022JE007680. [[CrossRef](#)]
82. Smith, M.R.; Bandfield, J.L.; Cloutis, E.A.; Rice, M.S. Hydrated Silica on Mars: Combined Analysis with near-Infrared and Thermal-Infrared Spectroscopy. *Icarus* **2013**, *223*, 633–648. [[CrossRef](#)]
83. Amador, E.S.; Bandfield, J.L. Elevated Bulk-Silica Exposures and Evidence for Multiple Aqueous Alteration Episodes in Nili Fossae, Mars. *Icarus* **2016**, *276*, 39–51. [[CrossRef](#)]
84. Rogers, A.D.; Nekvasil, H. Feldspathic Rocks on Mars: Compositional Constraints from Infrared Spectroscopy and Possible Formation Mechanisms: Feldspathic Rocks on Mars: Constraints. *Geophys. Res. Lett.* **2015**, *42*, 2619–2626. [[CrossRef](#)]
85. Cheek, L.C.; Pieters, C.M. Reflectance Spectroscopy of Plagioclase-Dominated Mineral Mixtures: Implications for Characterizing Lunar Anorthosites Remotely†. *Am. Mineral.* **2014**, *99*, 1871–1892. [[CrossRef](#)]
86. Collinet, M.; Médard, E.; Charlier, B.; Vander Auwera, J.; Grove, T.L. Melting of the Primitive Martian Mantle at 0.5–2.2 GPa and the Origin of Basalts and Alkaline Rocks on Mars. *Earth Planet. Sci. Lett.* **2015**, *427*, 83–94. [[CrossRef](#)]
87. Schmidt, M.E.; Campbell, J.L.; Gellert, R.; Perrett, G.M.; Treiman, A.H.; Blaney, D.L.; Ollila, A.; Calef, F.J.; Edgar, L.; Elliott, B.E.; et al. Geochemical Diversity in First Rocks Examined by the Curiosity Rover in Gale Crater: Evidence for and Significance of an Alkali and Volatile-Rich Igneous Source. *J. Geophys. Res. Planets* **2014**, *119*, 64–81. [[CrossRef](#)]
88. Dreibus, G.; Wanke, H. Mars, a Volatile-Rich Planet. *Meteoritics* **1985**, *20*, 367–381.
89. Reimink, J.R.; Chacko, T.; Stern, R.A.; Heaman, L.M. Earth’s Earliest Evolved Crust Generated in an Iceland-like Setting. *Nat. Geosci.* **2014**, *7*, 529–533. [[CrossRef](#)]
90. Nicholson, H.; Condomines, M.; Fitton, J.G.; Fallick, A.E.; Grönvold, K.; Rogers, G. Geochemical and Isotopic Evidence for Crustal Assimilation Beneath Krafla, Iceland. *J. Petrol.* **1991**, *32*, 1005–1020. [[CrossRef](#)]
91. Michalski, J.R.; Deanne Rogers, A.; Edwards, C.S.; Cowart, A.; Xiao, L. Diverse Volcanism and Crustal Recycling on Early Mars. *Nat. Astron.* **2024**, *8*, 456–462. [[CrossRef](#)]
92. Udry, A.; Balta, J.B.; McSween, H.Y. Exploring Fractionation Models for Martian Magmas: Fractionation of Martian Primary Magmas. *J. Geophys. Res. Planets* **2014**, *119*, 1–18. [[CrossRef](#)]
93. Payré, V.; Dasgupta, R. Effects of Phosphorus on Partial Melting of the Martian Mantle and Compositions of the Martian Crust. *Geochim. Cosmochim. Acta* **2022**, *327*, 229–246. [[CrossRef](#)]
94. Ding, S.; Dasgupta, R.; Tsuno, K. The Solidus and Melt Productivity of Nominally Anhydrous Martian Mantle Constrained by New High Pressure–Temperature Experiments—Implications for Crustal Production and Mantle Source Evolution. *J. Geophys. Res. Planets* **2020**, *125*, e2019JE006078. [[CrossRef](#)]
95. McCubbin, F.M.; Boyce, J.W.; Srinivasan, P.; Santos, A.R.; Elardo, S.M.; Filiberto, J.; Steele, A.; Shearer, C.K. Heterogeneous Distribution of H₂O in the Martian Interior: Implications for the Abundance of H₂O in Depleted and Enriched Mantle Sources. *Meteorit. Planet. Sci.* **2016**, *51*, 2036–2060. [[CrossRef](#)]
96. McCubbin, F.M.; Hauri, E.H.; Elardo, S.M.; Kaaden, K.E.V.; Wang, J.; Shearer, C.K. Hydrous Melting of the Martian Mantle Produced Both Depleted and Enriched Shergottites. *Geology* **2012**, *40*, 683–686. [[CrossRef](#)]
97. Seales, J.; Payre, V. Compositional Variations of Martian Primary Magmas Due to the Water Loss from the Martian Mantle. In Proceedings of the 52nd Lunar and Planetary Science Conference, Virtual, 15–19 March 2021; p. 2393.
98. Sandu, C.; Kiefer, W.S. Degassing History of Mars and the Lifespan of Its Magnetic Dynamo. *Geophys. Res. Lett.* **2012**, *39*, L03201. [[CrossRef](#)]

99. Knapmeyer-Endrun, B.; Bissig, F.; Compaire, N.; Joshi, R.; Garcia, R.; Khan, A.; Kim, D.; Lekic, V.; Margerine, L.; Panning, M.; et al. Seismic Constraints on the Crustal Structure of Mars from InSight Receiver Functions. In Proceedings of the 51st Lunar and Planetary Science Conference (2020), The Woodlands, TX, USA, 16–20 March 2020; Volume 51, p. 1914.
100. Manske, L.; Marchi, S.; Plesa, A.-C.; Wünnemann, K. Impact Melting upon Basin Formation on Early Mars. *Icarus* **2021**, *357*, 114128. [[CrossRef](#)]
101. Elkins-Tanton, L.T.; Zaranek, S.E.; Parmentier, E.M.; Hess, P.C. Early Magnetic Field and Magmatic Activity on Mars from Magma Ocean Cumulate Overturn. *Earth Planet. Sci. Lett.* **2005**, *236*, 1–12. [[CrossRef](#)]
102. Therriault, A.M.; Fowler, A.D.; Grieve, R.A.F. The Sudbury Igneous Complex: A Differentiated Impact Melt Sheet*. *Econ. Geol.* **2002**, *97*, 1521–1540. [[CrossRef](#)]
103. McEwen, A.S.; Eliason, E.M.; Bergstrom, J.W.; Bridges, N.T.; Hansen, C.J.; Delamere, W.A.; Grant, J.A.; Gulick, V.C.; Herkenhoff, K.E.; Keszthelyi, L.; et al. Mars Reconnaissance Orbiter’s High Resolution Imaging Science Experiment (HiRISE). *J. Geophys. Res.* **2007**, *112*, E05S02. [[CrossRef](#)]
104. Murchie, S.; Arvidson, R.E.; Bishop, J.L.; Calvin, W.M.; Carter, J.; Christian, J.; Clark, R.N.; Dundas, C.M.; Ehlmann, B.L.; Fox, V.K.; et al. Maximizing the Science and Resource Mapping Potential of Orbital VSWIR Spectral Measurements of Mars. *Bull. AAS* **2021**, *53*. [[CrossRef](#)]
105. Okada, T.; Fukuhara, T.; Tanaka, S.; Taguchi, M.; Imamura, T.; Arai, T.; Senshu, H.; Ogawa, Y.; Demura, H.; Kitazato, K.; et al. Thermal Infrared Imaging Experiments of C-Type Asteroid 162173 Ryugu on Hayabusa2. *Space Sci. Rev.* **2017**, *208*, 255–286. [[CrossRef](#)]
106. Christensen, P.R.; Hamilton, V.E.; Mehall, G.L.; Pelham, D.; O’Donnell, W.; Anwar, S.; Bowles, H.; Chase, S.; Fahlgren, J.; Farkas, Z.; et al. The OSIRIS-REx Thermal Emission Spectrometer (OTES) Instrument. *Space Sci. Rev.* **2018**, *214*, 87. [[CrossRef](#)]
107. Bapst, J.; Parker, T.J.; Balaram, J.; Tzanetos, T.; Matthies, L.H.; Edwards, C.D.; Freeman, A.; Withrow-Maser, S.; Johnson, W.; Amador-French, E.; et al. Mars Science Helicopter: Compelling Science Enabled by an Aerial Platform. *Bull. AAS* **2021**, *53*, 361. [[CrossRef](#)]
108. Rapin, W.; Maurice, S.; Ollila, A.; Wiens, R.C.; Dubois, B.; Nelson, T.; Le Men, C.; Parot, Y.; Clegg, S.; Newell, R.; et al. μ LIBS: A Micro-Scale Elemental Analyser for Lightweight In Situ Exploration. *LPSC* **2023**, *2806*, 1942.
109. Green, R.O.; Mouroulis, P.; Sullivan, P.; Bender, H.; Calvin, W.; Ehlmann, B.L.; Fraeman, A.A.; Thompson, D.R.; Vinckier, Q. Low-Cost, High Signal-to-Noise Ratio, and High Fidelity Imaging Spectrometers for Mars. In Proceedings of the Low-Cost Science Mission Concepts for Mars Exploration, Pasadena, CA, USA, 29–31 March 2022.
110. Debaille, V.; Yin, Q.-Z.; Brandon, A.D.; Jacobsen, B. Martian Mantle Mineralogy Investigated by the ^{176}Lu – ^{176}Hf and ^{147}Sm – ^{143}Nd Systematics of Shergottites. *Earth Planet. Sci. Lett.* **2008**, *269*, 186–199. [[CrossRef](#)]
111. Bonnet Gibet, V.; Michaut, C.; Bodin, T.; Wieczorek, M.; Dubuffet, F. Differentiation of the Martian Highlands during Its Formation. In Proceedings of the EGU General Assembly 2023, Vienna, Austria, 24–28 April 2023; p. EGU-2786. [[CrossRef](#)]
112. Barrat, J.-A.; Chaussidon, M.; Yamaguchi, A.; Beck, P.; Villeneuve, J.; Byrne, D.J.; Broadley, M.W.; Marty, B. A 4,565-My-Old Andesite from an Extinct Chondritic Protoplanet. *PNAS* **2021**, *118*, e2026129118. [[CrossRef](#)] [[PubMed](#)]
113. Collinet, M.; Grove, T.L. Widespread Production of Silica- and Alkali-Rich Melts at the Onset of Planetary Melting. *Geochim. Cosmochim. Acta* **2020**, *277*, 334–357. [[CrossRef](#)]
114. Barnes, J.J.; McCubbin, F.M.; Santos, A.R.; Day, J.M.D.; Boyce, J.W.; Schwenzer, S.P.; Ott, U.; Franchi, I.A.; Messenger, S.; Anand, M.; et al. Multiple Early-Formed Water Reservoirs in the Interior of Mars. *Nat. Geosci.* **2020**, *13*, 260–264. [[CrossRef](#)] [[PubMed](#)]
115. Michalski, J.R.; Rogers, A.D.; Edwards, C.S.; Cowart, A.; Xiao, L. Diverse Volcanism and Volcanotectonics Associated with the Eridania Basin on Mars. *LPSC* **2023**, *2806*, 1139.
116. Koepfel, A.H.D.; Black, B.A.; Marchi, S. Differentiation in Impact Melt Sheets as a Mechanism to Produce Evolved Magmas on Mars. *Icarus* **2020**, *335*, 113422. [[CrossRef](#)]
117. Mittelholz, A.; Heagy, L.; Johnson, C.L.; Bapst, J.; Espley, J.; Fraeman, A.A.; Langlais, B.; Lillis, R.; Rapin, W. Exploring Martian Magnetic Fields with a Helicopter. *Planet. Sci. J.* **2023**, *4*, 155. [[CrossRef](#)]
118. Smithies, R.H.; Lu, Y.; Johnson, T.E.; Kirkland, C.L.; Cassidy, K.F.; Champion, D.C.; Mole, D.R.; Zibra, I.; Gessner, K.; Sapkota, J.; et al. No Evidence for High-Pressure Melting of Earth’s Crust in the Archean. *Nat. Commun.* **2019**, *10*, 5559. [[CrossRef](#)] [[PubMed](#)]
119. Domagal-Goldman, S.D.; Wright, K.E.; Domagal-Goldman, S.D.; Wright, K.E.; Adamala, K.; Arina de la Rubia, L.; Bond, J.; Dartnell, L.R.; Goldman, A.D.; Lynch, K.; et al. The Astrobiology Primer v2.0. *Astrobiology* **2016**, *16*, 561–653. [[CrossRef](#)] [[PubMed](#)]

Disclaimer/Publisher’s Note: The statements, opinions and data contained in all publications are solely those of the individual author(s) and contributor(s) and not of MDPI and/or the editor(s). MDPI and/or the editor(s) disclaim responsibility for any injury to people or property resulting from any ideas, methods, instructions or products referred to in the content.